



OPEN

A mathematical-adapted model to analyze the characteristics for the mortality of COVID-19

Baobing Hao^{1,8}, Chengyou Liu^{2,8}✉, Yuhe Wang^{2,8}, Ninjun Zhu³, Yong Ding⁴, Jing Wu⁴, Yu Wang⁵, Fang Sun⁶✉ & Lixun Chen⁷✉

Severe acute respiratory syndrome coronavirus 2 (SARS-CoV-2) emerged in Wuhan, China, has led to the rapid development of Coronavirus disease 2019 (COVID-19) pandemic. COVID-19 represents a fatal disease with a great global public health importance. This study aims to develop a three-parameter Weibull mathematical model using continuous functions to represent discrete COVID-19 data. Subsequently, the model was applied to quantitatively analyze the characteristics for the mortality of COVID-19, including the age, sex, the length of symptom time to hospitalization time (SH), hospitalization date to death time (HD) and symptom time to death time time (SD) and others. A three-parameter mathematical model was developed by combining the reported cases in the Data Repository from the Center for Systems Science and Engineering at Johns Hopkins University and applied to estimate and analyze the characteristics for mortality of COVID-19. We found that the scale parameters of males and females were 5.85 and 5.45, respectively. Probability density functions in both males and females were negative skewness. 5% of male patients died under the age of 43.28 (44.37 for females), 50% died under 69.55 (73.25 for females), and 95% died under 86.59 (92.78 for females). The peak age of male death was 67.45 years, while that of female death was 71.10 years. The peak and median values of SH, HD and SD in male death were correspondingly 1.17, 5.18 and 10.30 days, and 4.29, 11.36 and 16.33 days, while those in female death were 1.19, 5.80 and 12.08 days, and 4.60, 12.44 and 17.67 days, respectively. The peak age of probability density in male and female deaths was 69.55 and 73.25 years, while the high point age of their mortality risk was 77.51 and 81.73 years, respectively. The mathematical model can fit and simulate the impact of various factors on IFR. From the simulation results of the model, we can intuitively find the IFR, peak age, average age and other information of each age. In terms of time factors, the mortality rate of the most susceptible population is not the highest, and the distribution of male patients is different from the distribution of females. This means that Self-protection and self-recovery in females against SARS-CoV-2 virus might be better than those of males. Males were more likely to be infected, more likely to be admitted to the ICU and more likely to die of COVID-19. Moreover, the infection fatality ration (IFR) of COVID-19 population was intrinsically linked to the infection age. Public health measures to protect vulnerable sex and age groups might be a simple and effective way to reduce IFR.

China was the first country to recognize the Coronavirus Disease 2019 (COVID-19), earlier termed as the 2019 Novel Coronavirus (2019-nCoV). Later, it was called SARS Cov-2, leading to severe acute respiratory syndrome. The main symptoms include fever, dry cough, fatigue, sore throat, loss of taste or smell, headache, diarrhea,

¹Department of Surgical Oncology, Jinling Hospital, School of Medicine, Nanjing University, Nanjing 210000, Jiangsu Province, China. ²Department of Medical Engineering, Nanjing First Hospital, Nanjing Medical University, No. 68, Changle Road, Qinhuai District, Nanjing City 210006, Jiangsu Province, China. ³Department of Neurology, Nanjing First Hospital, Nanjing Medical University, Nanjing 210006, Jiangsu Province, China. ⁴Department of Mathematics and Computer, Nanjing Medical University, Nanjing 210006, Jiangsu Province, China. ⁵Department of Medical Affairs, Nanjing First Hospital, Nanjing Medical University, 68 Changleroad, Nanjing 210006, Jiangsu Province, China. ⁶Department of Critical Care Medicine, Nanjing First Hospital, Nanjing Medical University, No. 68, Changle Road, Qinhuai District, Nanjing City 210006, Jiangsu Province, China. ⁷Department of Ophthalmology, Nanjing First Hospital, Nanjing Medical University, No. 68, Changle Road, Qinhuai District, Nanjing City 210006, Jiangsu Province, China. ⁸These authors contributed equally: Baobing Hao, Chengyou Liu and Yuhe Wang. ✉email: njfh_lchy@163.com; njfh_sunfang@163.com; njfh_chenlixun@163.com

difficulty of breathing, and/or chest pain. Many individuals were continuously and reportedly getting sick after being exposed from the virus. Due to its highly infective nature, the contagious disease spread across all Chinese provinces after almost a month. Concurrent with the nationwide spread, it also reached outside mainland China just after 13 day. Despite the great efforts made by China to contain the disease, it spread rapidly all over the world, causing an ongoing pandemic¹.

In January 2020, a study published in the *Lancet* indicated that COVID-19 symptoms first appeared on December 1, 2019². Many scholars believe that the virus originated in animals and spread by spillover infection^{3,4}. Professor Zhong Nanshan and the World Health Organization (WHO) confirmed human-to-human transmission of the virus on 20 January 2020⁵. According to official data from China, most cases of SARS-CoV-2 human-to-human transmission linked to the South China Seafood Wholesale Market⁶. In the early stages of the COVID-19 outbreak, the number of people diagnosed with COVID-19 doubled in about 7.5 days⁷. In January 2020, during the Chinese New Year, the rate of population migration increased dramatically, and SARS-CoV-2 began spreading to other Chinese cities⁸. By that time, official Chinese data indicated that 6,174 people in China had developed COVID-19 symptoms, but more suspected cases may have been infected^{9,10}. The personal protective equipment (PPE) was strongly recommended for health workers, according to a report published in the *Lancet* on 24 January 2020, citing the characteristics of human-to-human transmission of COVID-19^{11,12}. On January 30, 2020, when the WHO listed the COVID-19 epidemic as a Public Health Emergency of International Concern (PHEIC), the spread of SARS-CoV-2 increased nearly 200 times^{13,14}. On January 31, 2020, SARS-CoV-2 has spread to Italy and the first confirmed case of COVID-19 was announced¹⁵. As of March 13, 2020, WHO considered Europe to be the active epicenter of the pandemic¹⁶. On March 19, 2020, Italy became the country with the most COVID-19 deaths¹⁷. Up to March 26, the United States has replaced Italy and China as the country with the most confirmed cases of COVID-19¹⁸.

According to the National Health Commission of China, so far, COVID-19 has caused a total of 263,028,578 confirmed cases and 5,233,966 deaths worldwide. The mortality rate of confirmed cases in China was 5.2% (6697/127,938). Meanwhile, the mortality rate was 2.0% (5,227,269/262,900,640) among cases outside China. COVID-19 is highly infectious with a relatively high mortality rate. However, the messages obtainable in Internet reports and published studies are speedily increasing. In order to help medical workers around the world to better deal with COVID-19, we reviewed the relevant references and provided a general scenario mathematical model for relevant researchers, so as to prepare for the widespread epidemic of COVID-19.

Methods

Three-parameter Weibull data distribution model. Probability theory is the branch of mathematics concerned with probability. Although there are several different probability interpretations, probability theory adopts the concept in a rigorous mathematical manner through a set of axioms. It is a mathematical description of a random phenomenon in terms of its sample space and event probability (subsets of the sample space)¹⁹.

Survival analysis is a branch of probability theory, which is used for analyzing the expected duration of time until one or more events happen, such as death in biological organisms and failure in biological systems. This topic is called reliability theory or reliability analysis, and event history analysis in sociology. Survival analysis attempts to answer certain questions, such as what is the survival proportion of the population after a certain time? How quickly will those who survive die or fail? How does a particular situation or feature increase or decrease the probability of survival?

In probability theory and statistics, the Weibull distribution is a continuous probability distribution. It is named after Swedish mathematician Waloddi Weibull, who described it in detail in 1951, although it was first identified by Fréchet (1927) and first applied by Rosin & Rammler (1933) to describe a particle size distribution²⁰.

From the perspective of probability theory and statistics, the probability density function of a three-parameter Weibull data distribution model random variable is as follows:

$$f(t, \lambda, k, t_0) = \begin{cases} \frac{k}{\lambda} \left(\frac{t-t_0}{\lambda}\right)^{k-1} e^{-\left(\frac{t-t_0}{\lambda}\right)^k} & t \geq t_0 \\ 0 & t < t_0 \end{cases} \quad (1)$$

$k > 0$ is the shape parameter. $t_0 \geq 0$ is the location parameter. $\lambda > 0$ is the scale parameter of the function. Its complementary cumulative distribution function is a stretched exponential function. The Weibull distribution is related to the number of other probability distributions; In particular, it interpolates between the exponential distribution ($k = 1$) and the Rayleigh distribution ($k = 2, \lambda = \sqrt{2}\sigma$).

Cumulative distribution and reliability function. The reliability function of the Weibull data distribution model reflects the availability of the remaining lives of biological organisms. The definition of reliability function in reliability theory engineering is defined as the specific residual viability of biological organisms under specified conditions and time points. The cumulative density distribution function and reliability function can be calculated by Formula 1.

$$\begin{cases} F(t, \lambda, k, t_0) = \int_0^t f(\mu, \lambda, k, t_0) d\mu = e^{-\left(\frac{t-t_0}{\lambda}\right)^k} \\ R(t, \lambda, k, t_0) = 1 - F(t, \lambda, k, t_0) = 1 - e^{-\left(\frac{t-t_0}{\lambda}\right)^k} \end{cases} \quad (2)$$

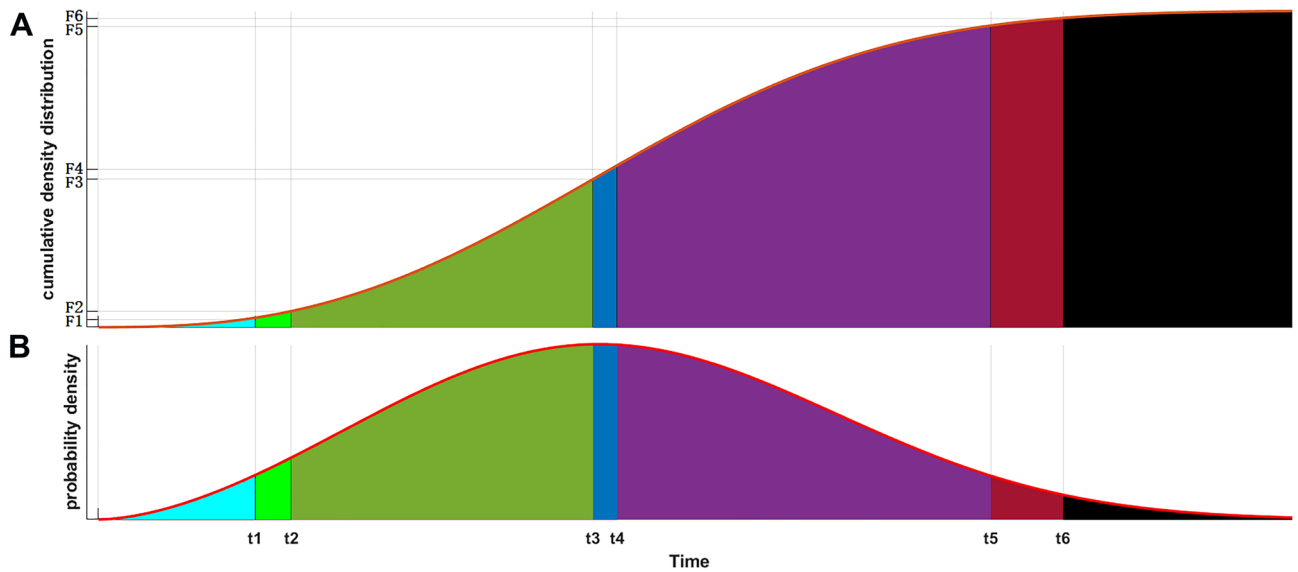


Figure 1. Calculation results of important time nodes. **(A)** Cumulative distribution function distribution. The abscissa is time. F1 = 2.5%, F2 = 5%, F4 = 50%, F5 = 95%, F6 = 97.5% and F3 is the Fpeak, which can be calculated by Figure B. **(B)** Probability density function distribution, in which t1 = T.lower 97.5% CI, t2 = T.lower 95% CI, t3 = T.peak, t4 = T.median, t5 = T.upper 95% CI and t6 = T.upper 97.5% CI.

According to the probability theory, important time nodes, such as “T.lower 95% CI” and “T.upper 95% CI”, “T.lower 97.5% CI” and “T.upper 97.5% CI”, “T.peak” and “T. median” (Fig. 1), can be calculated by the cumulative distribution function (Fig. 1).

$$T = \begin{bmatrix} \text{T.lower 97.5\% CI} \\ \text{T.lower 95\% CI} \\ \text{T.peak} \\ \text{T. median} \\ \text{T.upper 95\% CI} \\ \text{T.upper 97.5\% CI} \end{bmatrix} = t_0 - \lambda * \ln \left(\begin{bmatrix} \text{F.lower 97.5\% CI} \\ \text{F.lower 95\% CI} \\ \text{f.peak} \\ \text{f. median} \\ \text{F.upper 95\% CI} \\ \text{F.upper 97.5\% CI} \end{bmatrix} \right)^{\frac{1}{k}} \quad (3)$$

Ethics approval and consent to participate. Not applicable.

Patient consent for publication. Not applicable.

Estimation of Weibull data distribution model parameter

There are many methods to estimate the parameters of mathematical models, especially probability mathematical models. Commonly used methods include Gaussian estimation method, graphical method, least square method, maximum likelihood estimation method, etc.^{21–24} In this paper, we transformed the three-parameter Weibull data distribution model and used the maximum likelihood estimation method to estimate the model parameters.

Let $\psi = (\lambda, k, t_0)$. We used the logarithmic function to transform the three-parameter Weibull data distribution model. Let $M = \{t_1, t_2, t_3, \dots, t_n\}$. The model parameters were estimated as follows:

$$\begin{cases} \frac{\partial [\ln [L(\psi|M)]]}{\partial k} = \sum_{i=1}^n \left[\frac{1}{k} + \ln(t_i - t_0) - \ln \lambda - \left(\frac{t_i - t_0}{\lambda} \right)^k \ln \left(\frac{t_i - t_0}{\lambda} \right) \right] = 0 \\ \frac{\partial [\ln [L(\psi|M)]]}{\partial \lambda} = \sum_{i=1}^n \left[-\frac{k}{\lambda} + \frac{k(t_i - t_0)^k}{\lambda^{k+1}} \right] = 0 \\ \frac{\partial [\ln [L(\psi|M)]]}{\partial t_0} = \sum_{i=1}^n \left[-\frac{k-1}{t_i - t_0} + \frac{k(t_i - t_0)^{k-1}}{\lambda^k} \right] = 0 \end{cases} \quad (4)$$

Source of the COVID-19. The complete COVID-19 data set is a collection of COVID-19 data maintained by COVID-19 Data Repository by the CSSE at Johns Hopkins University (JHU) (<https://github.com/CSSEGISandData/COVID-19>). These data updated daily include numbers of confirmed cases, deaths, hospitalized cases, and testing cases, as well as other variables of potential interests, such as the age, sex, duration of symptoms, date of hospitalization, time of admission to ICU care, time of death, etc. The case & death data set is updated daily. The number of cases or deaths reported by any institution, including JHU, WHO, European

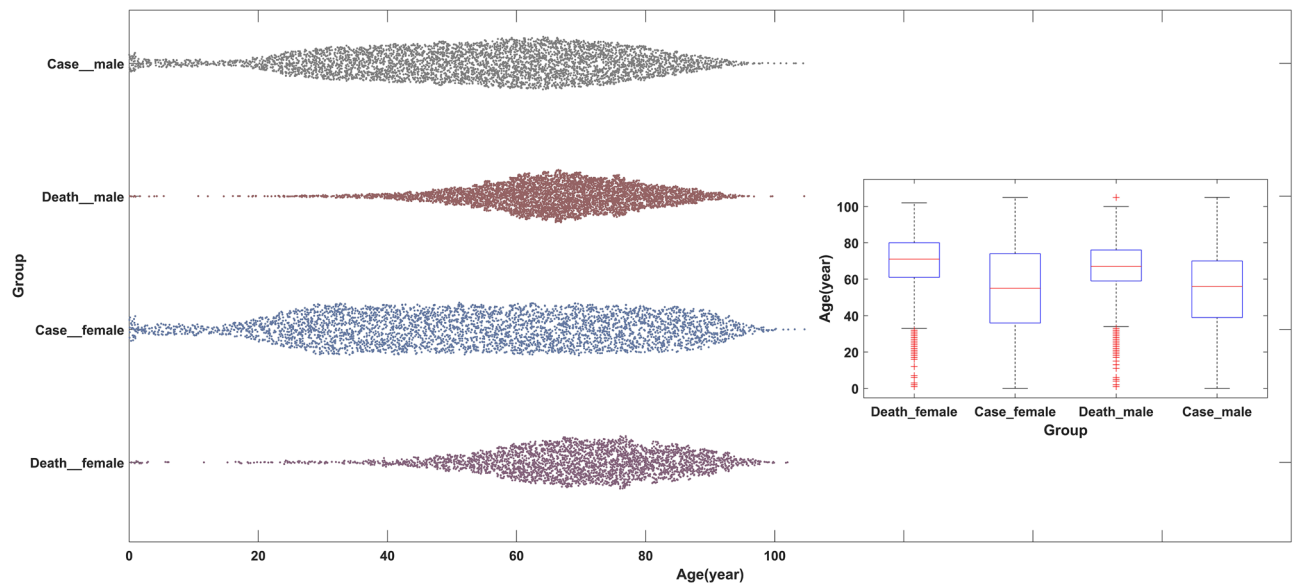


Figure 2. General characteristics and quality of COVID-19 cases. The scatter diagrams from the top to bottom were male cases who were infected with SARS-CoV-2 and hospitalized, male cases who were hospitalized and died, female cases who were infected with SARS-CoV-2 and hospitalized, and female cases who were hospitalized and died. The box plots from left to right corresponded to the scatter diagrams from the top to bottom.

Centre for Disease Prevention and Control (ECDC) and others, on a given day does not necessarily represent the actual number on that date.

Statement confirmation. All collected data were disclosed by the CSSE and validated by manual verification. The CSSE approved the waiver of informed consent. All data and materials are fully available without restriction. This study did not infringe on patient's privacy or health, and was performed according to the Declaration of Helsinki.

Result

General characteristics and quality of COVID-19 cases. The general characteristics and quality of COVID-19 about patients are shown in Fig. 2 and Table 1. As of the time of writing the manuscript, there were 88,911 hospitalizations caused by SARS-CoV-2 reported in CSSE, 14,529 patients in ICU and 8873 deaths in hospitals. Among the patients of COVID-19, 54.17% (48,162/88,911) were male, and 45.83% (40,749/88,911) were female. 59.01% (20,913/35,442) male cases and 40.99% (14,529/35,442) female cases who were sent to ICU, and 63.34% (5620/8873) male deaths and 36.66% (3253/8873) female deaths. At the same level, the proportion of male patients gradually increased (95% CI, $P < 0.01$). The impact of COVID-19 on the mortality differed from men and women. Among hospitalized cases, the mortality rate for males and females was 11.7% (5620/48,162) and 8.0% (3253/40,749), respectively, which was significantly higher in males with the ratio was 1.73:1 (95% CI, $P < 0.01$). The death age of males and females was normally distributed. Median death age was 66.5 years for males and 69.7 years for females. Variance age was 13.4 years for males and 15.2 years for females (95% CI, $P < 0.01$). 44.13% of hospitalizations occurred in patients over 70 years of age and 75.78% of deaths within that age bracket. The age distribution of hospitalized male and female cases tended to be uniform distributed, the median age of which was 54.2 years for males and 54.4 years for females. Meanwhile, the variance age was 20.8 years for males and 23.3 years for females (95% CI, $P = 0.45$).

Model calculations and fitting by age and sex based on deaths in hospital. The parameters of the three-parameter Weibull data distribution model were estimated by selecting the complete COVID-19 data set. The main variables were the age, sex, symptom time, hospitalization date, time of admission to ICU care, and death time. The calculation results of model parameters were shown in Table 2 and Fig. 3. Through the calculation results, for the age parameter, we found that the scale parameters of males and females who were infected and died, were 5.85 and 5.45, respectively. It is suggested that the probability density functions of the two groups were left-skewed curves, and females were more left-skewed (distribution with negative skewness) than males. At the same time, the location parameters of the two groups were 0.15 and 0.73, respectively, and the shape parameters of which were 71.67 and 75.29, respectively. For males, 63.2% died from 0.15 to 71.67 years, and for females, 63.2% died from 0.73 to 75.29 years.

Similarly, we calculated the model parameters using the symptom time, hospitalization date and death time. The results were shown in Table 2 and Fig. 3. In this paper, we defined the length of symptom time to hospitalization date as SH time, the length of hospitalization date to death time as HD time and the length of symptom

Age	Infected people who are hospitalized			Hospitalized people who go to Intensive Care Unit			Hospitalized people who die		
	Male	Female	Total	Male	Female	Total	Male	Female	Total
0–19	2553 (2.87)	2583 (2.91)	5136 (5.78)	1292 (3.65)	1086 (3.06)	2378 (6.71)	17 (0.19)	26 (0.29)	43 (0.48)
20–29	3773 (4.24)	4015 (4.52)	7788 (8.76)	708 (2.00)	578 (1.63)	1286 (3.63)	46 (0.52)	34 (0.38)	80 (0.90)
30–39	5863 (6.59)	5480 (6.16)	11,343 (12.76)	1036 (2.92)	663 (1.87)	1699 (4.79)	123 (1.39)	54 (0.61)	177 (1.99)
40–49	6847 (7.70)	5378 (6.05)	12,225 (13.75)	1848 (5.21)	1010 (2.85)	2858 (8.06)	367 (4.14)	176 (1.98)	543 (6.12)
50–59	7758 (8.73)	5425 (6.10)	13,183 (14.8)	3189 (8.99)	1640 (4.62)	4829 (13.6)	906 (10.2)	400 (4.50)	1306 (14.7)
60–69	8785 (9.88)	5457 (6.14)	14,242 (16.02)	4996 (14.10)	2585 (7.29)	7581 (21.39)	1769 (19.94)	812 (9.15)	2581 (29.09)
70–79	7321 (8.23)	5357 (6.03)	12,678 (14.26)	4609 (13.00)	3072 (8.67)	7681 (21.67)	1493 (16.83)	872 (9.83)	2365 (26.65)
80–89	4262 (4.79)	4867 (5.47)	9129 (10.27)	2689 (7.59)	2858 (8.06)	5547 (15.65)	765 (8.62)	637 (7.18)	1402 (15.80)
90+	1000 (1.12)	2187 (2.46)	3187 (3.58)	546 (1.54)	1037 (2.93)	1583 (4.47)	134 (1.51)	242 (2.73)	376 (4.24)
Total	48,162 (54.17)	40,749 (45.83)	88,911 (100.00)	20,913 (59.01)	14,529 (40.99)	35,442 (100.00)	5620 (63.34)	3253 (36.66)	8873 (100.00)

Table 1. Mathematical statistics calculation results by age and sex based on cases from CSSE. In Table 1, patients infected with SARS-CoV-2 were divided into six groups according to the sex, outcome and important time nodes. They were male/female cases who were infected with SARS-CoV-2 and hospitalized, male/female cases who were hospitalized and sent to ICU, and male/female cases who were hospitalized and died. According to age composition shown in Table 1, patients infected with SARS-CoV-2 were divided into 9 groups, including 0–19 years old group, 20–29 years old group, 30–39 years old group, 40–49 years old group, 50–59 years old group, 60–69 years old group, 70–79 years old group, 80–89 years old group and 90+ years old group.

Group		Model parameter			The important time nodes in the model						
		K	t0	λ	t1	t2	t3	t4	t5	t6	
Age groups	Male	71.67	0.15	5.85	38.38	43.28	69.55	67.45	86.59	89.72	
	Female	75.29	0.73	5.45	39.07	44.37	73.25	71.10	92.78	96.36	
Time nodes groups	Male	SH	5.81	0.04	1.17	0.30	0.50	1.17	4.29	14.89	17.77
		HD	14.89	0.08	1.32	1.00	1.65	5.18	11.36	34.27	40.11
		SD	20.66	0.09	1.52	1.93	3.02	10.30	16.33	42.62	48.86
	Female	SH	6.24	0.05	1.16	0.32	0.54	1.19	4.60	16.12	19.28
		HD	16.28	0.08	1.33	1.11	1.83	5.80	12.44	37.23	43.53
		SD	22.07	0.11	1.6	2.33	3.56	12.08	17.67	43.93	50.02

Table 2. The calculation results of model parameters and import time nodes. SH: the length of the symptom time to hospitalization date; HD: the length of the hospitalization date to death time; SD: the length of the symptom time to death time. t0: the location parameter; k: the shape parameter; λ : the scale parameter. t1 = T.lower 97.5% CI, t2 = T.lower 95% CI, t3 = T.peak, t4 = T.median, t5 = T.upper 95% CI and t6 = T.upper 97.5% CI.

time to death time as SD time. Through the model calculation, we found that the scale parameters of SH, HD and SD time for male patients were 1.17, 1.32 and 1.52, respectively. The scale parameters of SH, HD and SD time for female patients were 1.16, 1.33 and 1.60. In other words, all probability density curves were right-skewed (distribution with negative skewness). The shape parameters of SH, HD and SD for males were 5.81, 14.89, and 20.66, respectively, which were 6.24, 16.28 and 22.07 for females, respectively. Among death cases, 63.2% of male patients were hospitalized within 5.81 days (6.24 days of female patients) after symptom confirmation and died within 20.66 days (22.07 days of female patients).

As shown in Table 2, 2.5% males were hospitalized and died under 38.38 years (39.07 years of female patients), and 5% males were died under 43.28 years (44.37 years of female patients). Likewise, 5% males were died above the age of 86.59 years (92.78 years of female patients), and 2.5% males were died above the age of 89.72 years (96.36 years of female patients). The median age of males who died was 69.55 years (73.25 years of female patients). The mortality rate for males reached peak at 67.45 years (71.10 of females) SH, HD, SD time for males and females showed the same regular pattern (Table 2).

Influence of age risk factors on mortality. As shown in Fig. 4, it was evident that the mortality risk of COVID-19 for the elderly was many times higher than of the young. In fact, most COVID-19 deaths were

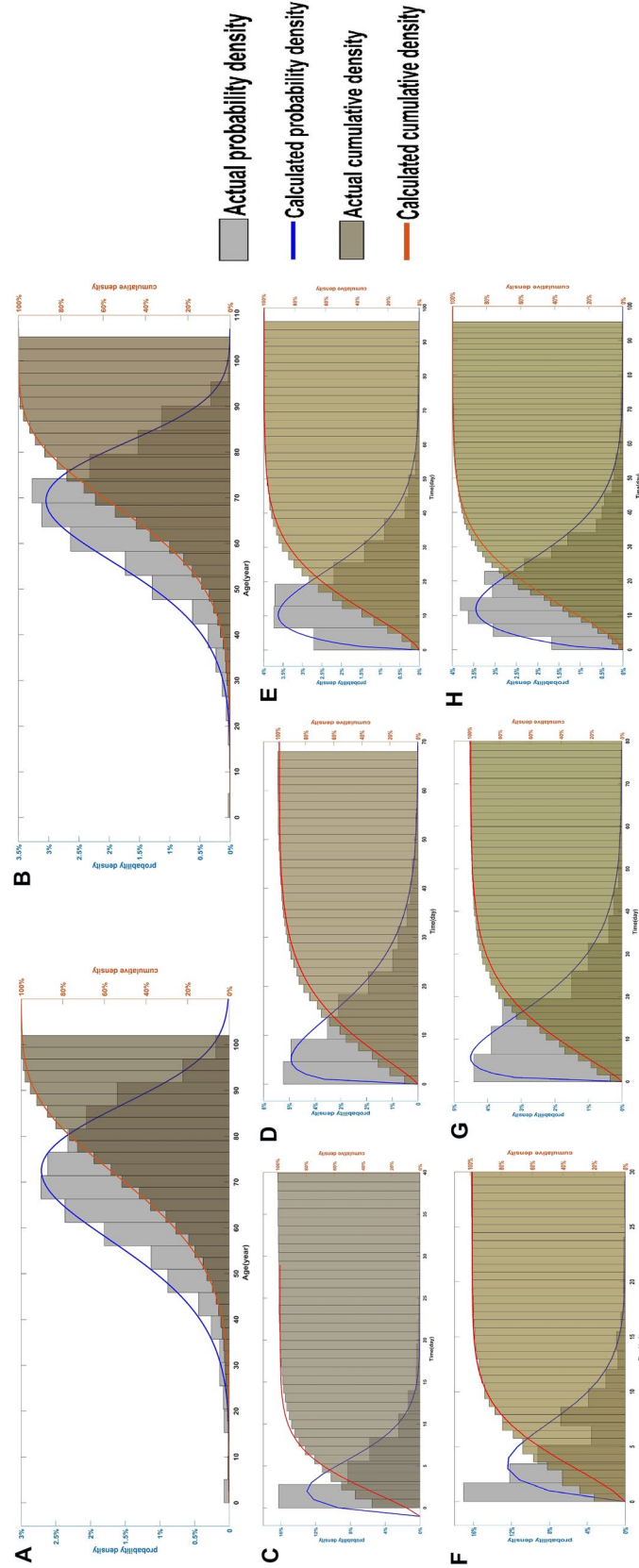


Figure 3. The results of model calculation used the COVID-19 data set. The gray histogram represented the actual probability density. The blue curve represented the calculated probability density, and the yellow curve represented the calculated cumulative density. The khaki histogram indicated the actual cumulative density. The blue histogram and blue curve were shown in principal coordinates, and the khaki histogram and yellow curve were shown in secondary coordinates. The results of model calculation used the (A) male and (B) female death data set. The results included the age at the death of male and female actual/calculated probability density and actual/calculated cumulative density. The models of (C) SH, (D) HD and (E) SD time for males, who were hospitalized and died, including SH, HD, SD time actual/calculated probability density and actual/calculated cumulative density. The models of (F) SH, (G) HD and (H) SD time for females, who were hospitalized and died, included SH, HD, SD time actual/calculated probability density and actual/calculated cumulative density.

elderly. In this article, 71.4% of male deaths and 76.6% of female deaths were older than 60 years old. Under the age of 40, the mortality risk of COVID-19 was lower. However, the mortality risk of deaths after 40 years of age increased rapidly, which reached highest at the age of 77.51 years. In addition, we found some interesting phenomena as follows. The highest mortality risk of female deaths was at the age of 81.73 years, while for male deaths was at the age of 77.51 years. For the influence of age factor, there was a significant difference between males and females on the mortality risk. In other words, the mortality risk for females was significantly later than that of males. For male deaths, although the peak age of death probability density was 69.55 years, the highest point age of mortality risk was 77.51 years. Similarly, the peak age of death probability density for females was 73.25 years, but the maximum point age of mortality risk was 81.73 years.

Discussion and conclusion

A review of COVID-19 epidemiological data showed that there were gender differences in COVID-19 disease. Compared with other countries, male COVID-19 in China and Italy have higher mortality rates^{25–27}. According to official Chinese data, the mortality rate for men was 2.8% and women was 1.7%²⁸. Male lifestyle, such as smoking and alcohol consumption, may be the main factor behind the difference in mortality rates between men and women with COVID-19 in China, according to an epidemiological review. From the immunological point of view, bad habits such as smoking and drinking may be the main causes of hypertension, cardiovascular and lung cancer, and may also be the main factors leading to higher male mortality^{29,30}. Official data in Europe have similar conclusions, men were more likely to be infected (57%), and also more likely to die (72%)³¹.

There were many key indicators, such as mortality rate (MR), case fatality rate (CFR) and infection rate (IFR), etc., which can be used to judge the severity of COVID-19³². Among these indicators, IFR was the most widely used and was used for explosive infectious diseases. IFR represented the percentage of deaths of all infected people, including those who died asymptomatic and undiagnosed. However, these key indicators were limited by differences in time, quality of the health care system, age and gender and other factors.

At the early stage of COVID-19 outbreak, IFR reported by WHO was below 1%^{33,34}. In August 2020, the chief scientist of WHO pointed that if the results of broad serology testing in Europe were included in the study, the IFR estimate was evaluated to converge between about 0.5% and 1%³⁵. In September 2020, the U.S. Centers for Disease Control and Prevention conducted the first age-specific IFR study for public health programs³⁶. In December 2020, a review and meta-analysis displayed that IFR was converge between 0.5 and 1% in many countries (Portugal, France, etc.), more than 2% in Italy, and between 1 and 2% in others (UK, Spain, etc.)³⁷. The study also pointed that the differences in IFR indirectly reflected the differences in disease infection rates among different age groups. The IFR value of younger adults and children was very low (e.g., 0.002% at age 10 and 0.01% at age 25). However, with the increase of age, IFR increased faster. For example, at the age of 55, the IFR was 0.4% (e.g., 1.4% at age 65 and 15% at age 85). These results were also highlighted in a December 2020 report issued by the WHO³⁸.

In this article, we proposed a three-parameter Weibull model to fit the COVID-19 data set, including age, sex, symptom time, hospitalization date, time of admission to ICU care, death time. At the same time, we could intuitively use continuous functions to qualitatively expressed continuous data. Overall, males infected by SARS-CoV-2 were more dangerous than females. Male-to-female ratios of hospitalized patients, ICU patients, and died patients were 1.18:1 (48,162:40,749), 1.22:1 (20,913:14,529) and 1.73:1 (5620:3253). Through calculation, for the patients who died from COVID-19, we found that the scale parameters of males and females were 5.85 and 5.45, location parameters were 0.15 and 0.73, and shape parameters were 71.67 and 75.29. Both probability density functions of males and females were negative skewness distributions, and females were more left-skewed than males. Further calculations indicated that 5% of males died under the age of 43.28 (44.37 for females), 50% died under 69.55 (73.25 for females), and 95% died under 86.59 (92.78 for females). In addition, the peak age of death in males was 67.45 years old, while that of females was 71.10 years old. In fact, the ages of male and female death were 66.5 ± 13.4 and 69.7 ± 15.2 years. From these results, we found that males were more likely to be infected, more likely to be admitted to the ICU and more likely to die, and the death age was generally younger than females. Those conclusions were similar to the comments of many scholars in the world^{39,40}. These findings suggested that it might be attributable to work style choices such as heavy workload, dangerous working environment, lifestyle choices such as smoking and drinking alcohol. In the early stages of the pandemic, the observation that males were more susceptible to COVID-19 was speculated to be due to gender differences in social behavior. Males were more likely to downplay the risk of COVID-19, ignoring preventive advices such as social distancing and wearing masks, and participating in mid-high-risk activities such as public gatherings.

In addition, we obtained some unexpected phenomena in this study. For example, the peak value of SH for male deaths was 1.17 days (1.19 days for females), and the median value was 4.29 days (4.60 days for females). Similarly, the peak values for males and females were 5.18 and 5.80 days, and the median values were 11.36 and 12.44 days. The peak values for males and females were 10.30 and 12.08 days, and the median values were 16.33 and 17.67 days, respectively. Both the peak values and median values of SH, HD and SD time, female were longer than those of males. However, the mortality rate of female was significantly lower than that of male, suggesting after being infected with the SARS-CoV-2 virus, females received treatment more later and had a longer struggle with the SARS-CoV-2 virus, but had a higher probability of survival than that of males. It is also indicated that self-protection and self-recovery against SARS-CoV-2 virus in females might be better than those of males. In fact, it was consistent with the situation observed in previous SARS-CoV and MERS-CoV (or other large-scale infectious diseases) infections. Moreover, in the COVID-19 data set, we found that for both male and female deaths, the peak risk age of death data was greater than the peak age of the probability density of deaths, and the peak risk age of males was smaller than that of females. This showed that the population IFR was intrinsically linked to the specific age group of infection. Therefore, in order to reduce the overall IFR, public health measures

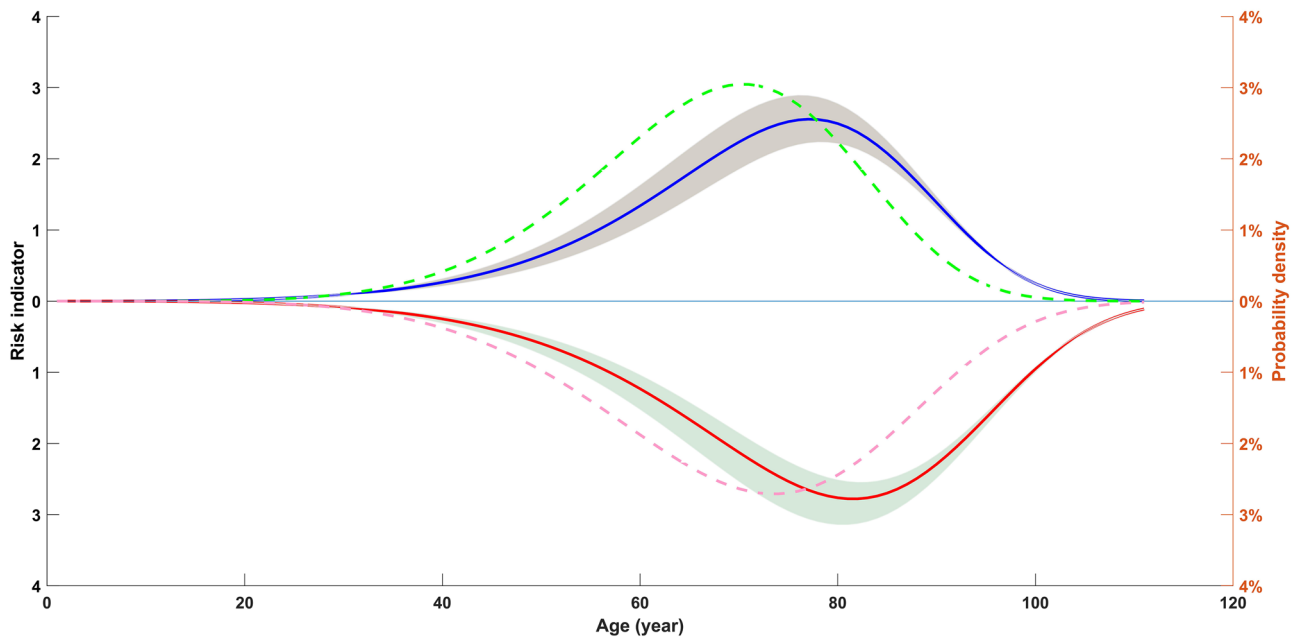


Figure 4. Influence of age risk factors on mortality. The green dotted line indicated the probability density of male death, and pink dotted line indicated female death. The blue line denoted the regression estimate of male mortality risk as a function of age, and red line denoted female mortality risk. The shaded region depicted the 95% confidence interval of the estimation.

to protect vulnerable sex and age groups may be a simple and effective measure. For example, when the amount of vaccine is severely insufficient, giving priority to the distribution of vaccines according to sex and age groups may be the most important public health measure.

However, general behaviour (habits) and biological factors (immune response) can determine the consequences of COVID-19⁴¹. Many of those who die of COVID-19 have pre-existing conditions, including hypertension, diabetes mellitus, and cardiovascular disease, etc.⁴² According to the CDC report, the most common comorbidities of COVID-19 are respiratory syndrome, including moderate or severe asthma, pre-existing COPD, pulmonary fibrosis, cystic fibrosis⁴³. When someone with existing comorbidities problems is infected with COVID-19, they might be at greater risk for severe symptoms. When completing this continuous mathematical model, we realized the limitations of this study. This model can be used to explain the general continuity problems, including exponential distribution, Rayleigh distribution, normal distribution, partial normal distribution, average distribution, but cannot be used to explain the discrete (comorbidities) problems. This question will be the focus of our research.

Availability of data and materials

The complete COVID-19 data set is a collection of the COVID-19 data maintained by COVID-19 Data Repository by the Center for Systems Science and Engineering (CSSE) at Johns Hopkins University (<https://github.com/CSSEGISandData/COVID-19>). All data and materials are fully available without restriction.

Received: 1 July 2021; Accepted: 14 March 2022

Published online: 31 March 2022

References

- Lin, X., Rocha, I. C. N., Shen, X., Ahmadi, A. & Lucero-Prisno, D. E. Challenges and strategies in controlling COVID-19 in mainland China: Lessons for future public health emergencies. *J. Soc. Health* **4**, 57–61 (2021).
- Andersen, K. G., Rambaut, A., Lipkin, W. I., Holmes, E. C. & Garry, R. F. The proximal origin of SARS-CoV-2. *Nat. Med.* **26**, 450–452. <https://doi.org/10.1038/s41591-020-0820-9> (2020).
- Chan, K. W., Wong, V. T. & Tang, S. C. W. COVID-19: An update on the epidemiological, clinical, preventive and therapeutic evidence and guidelines of integrative Chinese-Western medicine for the management of 2019 novel coronavirus disease. *Am. J. Chin. Med.* **48**, 737–762. <https://doi.org/10.1142/S0192415X20500378> (2020).
- Sun, S. *et al.* COVID-19 and healthcare system in China: Challenges and progression for a sustainable future. *Glob. Health* **17**, 14. <https://doi.org/10.1186/s12992-021-00665-9> (2021).
- Baghizadeh, F. M. What dentists need to know about COVID-19. *Oral. Oncol.* **105**, 104741. <https://doi.org/10.1016/j.oraloncology.2020.104741> (2020).
- Chinese Center for Disease Control and Prevention. Guidelines for COVID-19 Epidemiological Investigations. *China CDC Wkly.* **2**, 327–328. <https://doi.org/10.46234/ccdcw2020.083> (2020).
- Li, Q. *et al.* Early transmission dynamics in Wuhan, China, of novel coronavirus-infected pneumonia. *N. Engl. J. Med.* **382**, 1199–1207. <https://doi.org/10.1056/NEJMoa2001316> (2020).

8. Peng, T., Liu, X., Ni, H., Cui, Z. & Du, L. City lockdown and nationwide intensive community screening are effective in controlling the COVID-19 epidemic: Analysis based on a modified SIR model. *PLoS One*. **15**, e0238411. <https://doi.org/10.1371/journal.pone.0238411> (2020).
9. Li, H. *et al.* Coronavirus disease 2019 (COVID-19): Current status and future perspectives. *Int. J. Antimicrob. Agents* **55**, 105951. <https://doi.org/10.1016/j.ijantimicag.2020.105951> (2020).
10. Yamayoshi, S. *et al.* Comparison of rapid antigen tests for COVID-19. *Viruses* **12**, 1420. <https://doi.org/10.3390/v12121420> (2020).
11. Huang, C. *et al.* Clinical features of patients infected with 2019 novel coronavirus in Wuhan, China. *Lancet* **395**, 497–506. [https://doi.org/10.1016/S0140-6736\(20\)30183-5](https://doi.org/10.1016/S0140-6736(20)30183-5) (2020).
12. Wollina, U. Challenges of COVID-19 pandemic for dermatology. *Dermatol. Ther.* **33**, e13430. <https://doi.org/10.1111/dth.13430> (2020).
13. Kim, J. H., Marks, F. & Clemens, J. D. Looking beyond COVID-19 vaccine phase 3 trials. *Nat. Med.* **27**, 205–211. <https://doi.org/10.1038/s41591-021-01230-y> (2021).
14. Han, Y., Lie, R. K. & Guo, R. The internet hospital as a telehealth model in China: Systematic search and content analysis. *J. Med. Internet Res.* **22**, e17995. <https://doi.org/10.2196/17995> (2020).
15. Pierri, M. D., Alfonsi, J., Cefarelli, M., Berretta, P. & Di, E. M. COVID 19—perspective of an Italian Center. *J. Card. Surg.* **36**, 1696–1702. <https://doi.org/10.1111/jocs.15099> (2021).
16. Awan, T. M. & Aslam, F. Prediction of daily COVID-19 cases in European countries using automatic ARIMA model. *J. Public Health Res.* **9**, 1765. <https://doi.org/10.4081/jphr.2020.1765> (2020).
17. Grasselli, G. *et al.* Risk factors associated with mortality among patients with COVID-19 in intensive care units in Lombardy, Italy. *JAMA Intern. Med.* **180**, 1345–1355. <https://doi.org/10.1001/jamainternmed.2020.3539> (2020).
18. Tai, D. B. G., Shah, A., Doubeni, C. A., Sia, I. G. & Wieland, M. L. The disproportionate impact of COVID-19 on racial and ethnic minorities in the United States. *Clin Infect Dis.* **72**, 703–706. <https://doi.org/10.1093/cid/ciaa815> (2021).
19. Costello, F. & Watts, P. Probability theory plus noise: Descriptive estimation and inferential judgment. *Top. Cogn. Sci.* **10**, 192–208. <https://doi.org/10.1111/tops.12319> (2018).
20. Juckett, D. A. & Rosenberg, B. Comparison of the Gompertz and Weibull functions as descriptors for human mortality distributions and their intersections. *Mech Ageing Dev.* **69**, 1–31. [https://doi.org/10.1016/0047-6374\(93\)90068-3](https://doi.org/10.1016/0047-6374(93)90068-3) (1993).
21. Vetter, T. R. Fundamentals of research data and variables: The devil is in the details. *Anesth. Analg.* **125**, 1375–1380. <https://doi.org/10.1213/ANE.0000000000002370> (2017).
22. Perera, R., Heneghan, C. & Yudkin, P. Graphical method for depicting randomised trials of complex interventions. *BMJ* **334**, 127–129. <https://doi.org/10.1136/bmj.39045.396817.68> (2007).
23. Ojima, J. Airflow equation of a slot hood by the least square method. *Sangyo Eiseigaku Zasshi* **54**, 108–113. <https://doi.org/10.1539/sangyoeisei.b12001> (2012).
24. Lim, S., Tellez, M. & Ismail, A. I. Estimating a dynamic effect of soda intake on pediatric dental caries using targeted maximum likelihood estimation method. *Caries Res.* **53**, 532–540. <https://doi.org/10.1159/000497359> (2019).
25. Chen, N. *et al.* Epidemiological and clinical characteristics of 99 cases of 2019 novel coronavirus pneumonia in Wuhan, China: A descriptive study. *Lancet* **395**, 507–513. [https://doi.org/10.1016/S0140-6736\(20\)30211-7](https://doi.org/10.1016/S0140-6736(20)30211-7) (2020).
26. Wenham, C., Smith, J. & Morgan, R. Gender and COVID-19 Working Group. COVID-19: The gendered impacts of the outbreak. *Lancet* **395**, 846–848. [https://doi.org/10.1016/S0140-6736\(20\)30526-2](https://doi.org/10.1016/S0140-6736(20)30526-2) (2020).
27. Epidemiology Working Group for NCIP Epidemic Response, Chinese Center for Disease Control and Prevention. The epidemiological characteristics of an outbreak of 2019 novel coronavirus diseases (COVID-19) in China. *Zhonghua Liu Xing Bing Xue Za Zhi* **41**, 145–151. <https://doi.org/10.3760/cma.j.issn.0254-6450.2020.02.003> (2020).
28. Jiang, F. *et al.* Review of the clinical characteristics of coronavirus disease 2019 (COVID-19). *J. Gen. Intern. Med.* **35**, 1545–1549. <https://doi.org/10.1007/s11606-020-05762-w> (2020).
29. Wiersinga, W. J., Rhodes, A., Cheng, A. C., Peacock, S. J. & Prescott, H. C. Pathophysiology, transmission, diagnosis, and treatment of coronavirus disease 2019 (COVID-19): A review. *JAMA* **324**, 782–793. <https://doi.org/10.1001/jama.2020.12839> (2020).
30. Borghesi, A. & Maroldi, R. COVID-19 outbreak in Italy: Experimental chest X-ray scoring system for quantifying and monitoring disease progression. *Radiol. Med.* **125**, 509–513. <https://doi.org/10.1007/s11547-020-01200-3> (2020).
31. Gebhard, C., Regitz, Z. V., Neuhauser, H. K., Morgan, R. & Klein, S. L. Impact of sex and gender on COVID-19 outcomes in Europe. *Biol. Sex Differ.* **11**, 29. <https://doi.org/10.1186/s13293-020-00304-9> (2020).
32. Lee, S. H. *et al.* Physiologic characteristics and clinical outcomes of patients with discordance between FFR and iFR. *JACC Cardiovasc. Interv.* **12**, 2018–2031. <https://doi.org/10.1016/j.jcin.2019.06.044> (2019).
33. Xiong, J. *et al.* Impact of COVID-19 pandemic on mental health in the general population: A systematic review. *J. Affect. Disord.* **277**, 55–64. <https://doi.org/10.1016/j.jad.2020.08.001> (2020).
34. Meyerowitz, K. G. & Merone, L. A systematic review and meta-analysis of published research data on COVID-19 infection fatality rates. *Int. J. Infect. Dis.* **101**, 138–148. <https://doi.org/10.1016/j.ijid.2020.09.1464> (2020).
35. Rawaf, S. *et al.* Lessons on the COVID-19 pandemic, for and by primary care professionals worldwide. *Eur. J. Gen. Pract.* **26**, 129–133. <https://doi.org/10.1080/13814788.2020.1820479> (2020).
36. Wallace, M. *et al.* COVID-19 in correctional and detention facilities—United States, February–April 2020. *MMWR Morb. Mortal. Wkly. Rep.* **69**, 587–590. <https://doi.org/10.15585/mmwr.mm6919e1> (2020).
37. Levin, A. T. *et al.* Assessing the age specificity of infection fatality rates for COVID-19: Systematic review, meta-analysis, and public policy implications. *Eur. J. Epidemiol.* **35**, 1123–1138. <https://doi.org/10.1007/s10654-020-00698-1> (2020).
38. Wang, K. *et al.* Intention of nurses to accept coronavirus disease 2019 vaccination and change of intention to accept seasonal influenza vaccination during the coronavirus disease 2019 pandemic: A cross-sectional survey. *Vaccine* **38**, 7049–7056. <https://doi.org/10.1016/j.vaccine.2020.09.021> (2020).
39. Hu, Y. *et al.* Prevalence and severity of corona virus disease 2019 (COVID-19): A systematic review and meta-analysis. *J. Clin. Virol.* **127**, 104371. <https://doi.org/10.1016/j.jcv.2020.104371> (2020).
40. Fu, L. *et al.* Clinical characteristics of coronavirus disease 2019 (COVID-19) in China: A systematic review and meta-analysis. *J. Infect.* **80**, 656–665. <https://doi.org/10.1016/j.jinf.2020.03.041> (2020).
41. Lu, J. *et al.* Clinical, immunological and virological characterization of COVID-19 patients that test re-positive for SARS-CoV-2 by RT-PCR. *EBioMedicine* **59**, 102960. <https://doi.org/10.1016/j.ebiom.2020.102960> (2020).
42. Garg, S. *et al.* Hospitalization rates and characteristics of patients hospitalized with laboratory-confirmed coronavirus disease 2019—COVID-NET, 14 States, March 1–30, 2020. *MMWR*. **69**, 458–464. <https://doi.org/10.15585/mmwr.mm6915e3> (2020).
43. Frutos, R., Gavotte, L. & Devaux, C. A. Understanding the origin of COVID-19 requires to change the paradigm on zoonotic emergence from the spillover to the circulation model. *Infect. Genet. Evol.* **95**, 104812. <https://doi.org/10.1016/j.meegid.2021.104812> (2020).

Acknowledgements

The authors thank Professor D. Y for help in data analysis. The authors thank Dr. J. W for suggestions and corrections that improved the text.

Author contributions

C.Y.L., B.B.H. and N.J.Z. contributed to article writing. Y.D. and J.W. were responsible for article technical guidance and article revision. L.X.C. and F.S. designed the study and guided the experiment. C.Y.L., Y.W. and Y.H.W. devoted themselves to data collection. All authors were responsible for experimental design and proofread the final version of manuscript.

Funding

This work has been supported by the Innovation Foundation of Nanjing Medical University (2014NJMU035).

Competing interests

The authors declare no competing interests.

Additional information

Supplementary Information The online version contains supplementary material available at <https://doi.org/10.1038/s41598-022-09442-z>.

Correspondence and requests for materials should be addressed to C.L., F.S. or L.C.

Reprints and permissions information is available at www.nature.com/reprints.

Publisher's note Springer Nature remains neutral with regard to jurisdictional claims in published maps and institutional affiliations.



Open Access This article is licensed under a Creative Commons Attribution 4.0 International License, which permits use, sharing, adaptation, distribution and reproduction in any medium or format, as long as you give appropriate credit to the original author(s) and the source, provide a link to the Creative Commons licence, and indicate if changes were made. The images or other third party material in this article are included in the article's Creative Commons licence, unless indicated otherwise in a credit line to the material. If material is not included in the article's Creative Commons licence and your intended use is not permitted by statutory regulation or exceeds the permitted use, you will need to obtain permission directly from the copyright holder. To view a copy of this licence, visit <http://creativecommons.org/licenses/by/4.0/>.

© The Author(s) 2022